



Low-metallicity AGB models: the H profile in the ^{13}C -pocket and the effect on the s -process

S. Bisterzo¹ and S. Cristallo^{2,3}

¹ Dipartimento di Fisica Generale, Università di Torino, 10125 (To) Italy
e-mail: bisterzo@ph.unito.it

² Departamento de Física Teórica y del Cosmos, Universidad de Granada, Campus de Fuentenueva, 18071 Granada, Spain

³ INAF Osservatorio Astronomico di Collurania, via M. Maggini, 64100 Teramo, Italy

Abstract. The $^{13}\text{C}(\alpha, n)^{16}\text{O}$ reaction is the major neutron source in low-mass asymptotic giant branch (AGB) stars, where the main and the strong s -process components are synthesised. After a third dredge-up (TDU) episode, ^{13}C burns radiatively, in a thin pocket which forms in the top layers of the He-intershell, by proton capture on the abundant ^{12}C . Therefore, mixing of a few protons from the H-rich envelope into the He-rich region is required. However, the origin and the efficiency of this mixing episode are still matters for debate and, consequently, the formation of the ^{13}C -pocket represents a significant source of uncertainty that affects AGB models. We analyse the effects on the nucleosynthesis of the s -elements caused by the variation of the hydrogen profile in the region where the ^{13}C -pocket forms for an AGB model with $M = 2 M_{\odot}$ and $[\text{Fe}/\text{H}] = -2.3$. In particular, we concentrate on three isotopes (^{89}Y , ^{139}La and ^{208}Pb), chosen as representative of the three s -process peaks.

Key words. Stars: C and s rich – Stars: abundances – Stars: nucleosynthesis

1. Introduction

During their thermally pulsing (TP) phase, low-mass asymptotic giant branch (AGB) stars are the site of the main and the strong component of the s -process, which is responsible for the nucleosynthesis of half the nuclei from Sr to Pb/Bi. After a limited number of pulses, the convective envelope penetrates into the He-intershell at the quenching of each convective instability, mixing freshly synthesized ^4He , ^{12}C and s -process elements to the surface (third dredge-up, TDU).

The major neutron source in low-mass AGB stars is the $^{13}\text{C}(\alpha, n)^{16}\text{O}$ reaction, which burns radiatively during the interpulse period in a thin region at the top of the He-intershell (^{13}C -pocket). The physical mechanism that allows the formation of the ^{13}C -pocket is debated. A small number of protons are assumed to penetrate from the envelope into the He-intershell during TDU episodes (Iben & Renzini 1982). Then, at H reignition, a large amount of ^{13}C is synthesised in the top layers of the intershell by the $^{12}\text{C}(p, \gamma)^{13}\text{N}(\beta^+ \nu)^{13}\text{C}$ nuclear chain. This ^{13}C is of primary origin and, therefore, independent of the metallicity. During the interpulse, the H-burning shell ad-

vances in mass, compressing and heating the underlying material, and at $T \approx 0.9 \times 10^8$ K the $^{13}\text{C}(\alpha, n)^{16}\text{O}$ reaction starts releasing neutrons in radiative conditions. Later on, the synthesised s -process nuclei are engulfed and diluted in the next convective region generated by TP.

Different evolutionary and post-processing codes have been developed in recent years to understand nucleosynthesis in low-mass AGB stars (e.g. Straniero et al. 1995, 2003; Gallino et al. 1998; Goriely & Mowlavi 2000; Karakas & Lattanzio 2003, 2007; Campbell & Lattanzio 2008; Straniero et al. 2006). Several mechanisms have been proposed to reproduce the mixing leading to the ^{13}C -pocket formation. These include semi-convection, models with rotation (Langer et al. 1999; Herwig et al. 2003; Siess et al. 2004), gravity waves (Denissenkov & Tout 2003), exponential diffusive overshooting at the borders of all convective zones (Herwig et al. 1997) and opacity-induced overshooting at the base of the convective envelope (Straniero et al. 2006). A clear answer to the properties of such mixing has not been reached yet.

We test here the effects on the nucleosynthesis of the s elements by adopting different H profiles in the region of the ^{13}C -pocket forming after the first TDU of an AGB model with initially $M = 2 M_{\odot}$ and $[\text{Fe}/\text{H}] = -2.3$. Comparison between the full evolutionary FRANECS (Frascati Raphson-Newton Evolutionary Code) models (Cristallo et al. 2009, hereinafter C09) and FRANECS models coupled with a post-processing nucleosynthesis method (Gallino et al. 1998; Bisterzo et al. 2010) are presented.

2. Results

C09 introduce a mixing algorithm which depends on a free parameter¹ in their full evolutionary models to mimic the formation of a transition zone between the fully convective envelope and the radiatively stable H-exhausted core. Thus, a partial mixing of protons takes place and leads to the formation of

¹ See C09 for the procedure followed to calibrate it.

a ^{13}C rich layer. Its mass and profile decrease with the number of pulses (see C09, their figs 4 and 8).

Fig. 1, top panel, shows this region. In the uppermost layers of the pocket, where protons are more abundant, the ^{13}C -pocket overlaps with a ^{14}N -pocket, which forms via the $^{13}\text{C}(p, \gamma)^{14}\text{N}$ reaction. ^{14}N acts as a neutron poison via the resonant reaction $^{14}\text{N}(n, p)^{14}\text{C}$. Thus by subtracting neutrons from the nucleosynthesis of the s -process elements. Fig. 1, bottom panel, shows the same mass region at the end of the ^{13}C burning. We concentrate on three isotopes, ^{89}Y , ^{139}La and ^{208}Pb , chosen as representative of the three s -process peaks. As expected, at this low metallicity, a large amount of ^{208}Pb is produced (Gallino et al. 1998). Maximum Pb production occurs in the central layers of the pocket where $X(^{13}\text{C}) > X(^{14}\text{N})$ (we find $X(^{208}\text{Pb}) = 4.5 \times 10^{-5}$), while Y and La show definitely lower abundances: $X(^{89}\text{Y}) \approx X(^{139}\text{La}) \approx 6 \times 10^{-9}$. In the outer and inner regions of the pocket, however, ^{89}Y and ^{139}La show peaked distributions. Note that, in the outer tail, s -process elements are efficiently synthesised even if $X(^{13}\text{C}) < X(^{14}\text{N})$.

In order to test the effect of these tails on Y, La and Pb with different H profiles, we use the post-processing nucleosynthesis models described by Bisterzo et al. (2010). We adopt the H profile of Gallino et al. (1998, case ST, their fig. 2). Then we introduce a further region in the pocket (with mass $M = 4 \times 10^{-4} M_{\odot}$) in which we change the abundances of ^{13}C and ^{14}N to simulate different H profiles in the tails. We multiply or divide by different factors the ^{13}C and ^{14}N abundances in the pocket². Note that the H profile and the mass of the pocket are kept constant pulse by pulse. The envelope abundances of the two s -process indices $[\text{La}/\text{Y}]$ and $[\text{Pb}/\text{La}]$ obtained with the post-processing method are shown in Tables 1 and 2. In Table 1, first group, we show the results computed with standard ^{13}C -pockets (with three zones as Gallino et al. 1998) for various ^{13}C -pocket efficiencies (from

² In fact a range of ^{13}C -pockets is introduced in order to interpret the spread in the s -elements observed in CEMP- s stars.

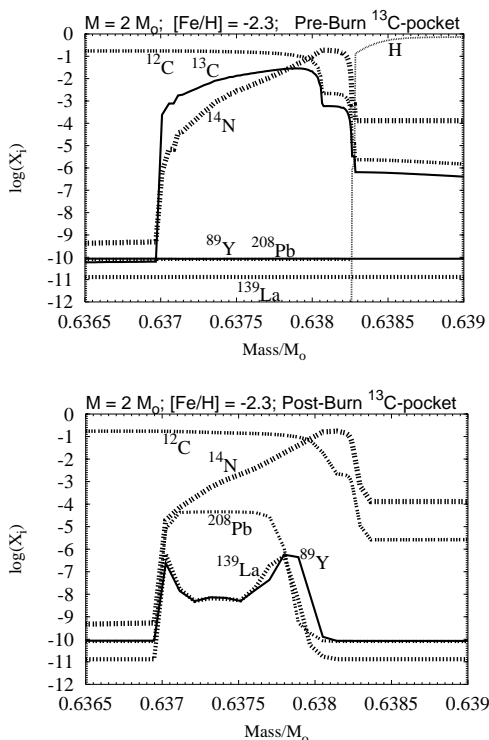


Fig. 1. ^{13}C -pocket mass region for a full evolutionary AGB model of $M = 2 M_{\odot}$ and $[\text{Fe}/\text{H}] = -2.3$ (C09) after the first TDU, at the pocket formation (top panel) and at the end of the ^{13}C burning (bottom panel).

ST $\times 2$ down to ST/24). These results are compared with models with an added fourth zone with $X(^{13}\text{C}) < X(^{14}\text{N})$ (Table 1, second group). This has been done to simulate the effect induced by the outer tail of the pocket shown in Fig. 1 by C09 model on post-processing calculation results. C09 obtain a final $[\text{La}/\text{Y}] = 0.45$ and $[\text{Pb}/\text{La}] = 1.30$. With the post-processing method and a range of standard ^{13}C -pockets, $[\text{La}/\text{Y}]$ reaches a maximum value of about 0.9 (case ST/6) and $[\text{Pb}/\text{La}] \approx 2.2$ (case ST/1.5). When adding the fourth zone, minimal variations are found for large and low ^{13}C -pocket efficiencies, while appreciable differences are found in the intermediate cases. For large ^{13}C abundances (case ST $\times 2$), the addition of fourth zone leads to a large production of light elements (Ne, Na and Mg) whose poisoning effect induces a slightly decrease in the final s -

process element surface overabundances. For very low ^{13}C efficiencies the s -process production is mainly due to the $^{22}\text{Ne}(\alpha, n)^{25}\text{Mg}$ reaction (Bisterzo et al. 2010). This minimizes the effects of additional ^{13}C and ^{14}N . For intermediate cases the introduction of the fourth zone instead reduces the maximum $[\text{La}/\text{Y}]$ to about 0.5 dex and the maximum $[\text{Pb}/\text{La}]$ to about 1.6 dex. In Table 2 we select the highest ^{13}C -pocket case (case ST $\times 2$) and we test the effect of an added fourth zone with different $X(^{13}\text{C})$ values (assuming $X(^{14}\text{N})$ is negligible). We choose the ST $\times 2$ case because previous comparisons done at larger metallicities (C09) indicate that the best agreement between post-processed and full evolutionary models is found with this case. The standard case with three zones only (column II) gives $[\text{La}/\text{Y}] = 0.50$ and $[\text{Pb}/\text{La}] = 2.04$, while the addition of a fourth zone with $X(^{13}\text{C}) = 3.8 \times 10^{-4}$ (test III) definitely lowers the $[\text{Pb}/\text{La}]$ ratio (to 1.47) leaving practically untouched the $[\text{La}/\text{Y}]$ ratio (at 0.56). Thus, a reasonable agreement between this test and C09 is found even at such low metallicities. After verifying that the tails of the ^{13}C -pocket affect the s distribution, one may constrain the choice of the H profile through a study of spectroscopic observations in CEMP- s stars. Note that, for disc metallicities, the tails of the pocket do not influence the s distribution noticeably.

3. Conclusions

The maximum amount of ^{13}C and ^{14}N in the pocket and different hydrogen profiles (and therefore the amount of ^{13}C and ^{14}N in the tails of the pocket) modify the s abundance distribution. In particular, the s -process indices $[\text{La}/\text{Y}]$ and $[\text{Pb}/\text{La}]$ are sensitive to the tails of the pocket. At $[\text{Fe}/\text{H}] = -2.3$ a large amount of ^{208}Pb is produced when $X(^{13}\text{C}) > X(^{14}\text{N})$. A first interesting consequence caused by the addition of an outer tail in the pocket with $X(^{13}\text{C}) < X(^{14}\text{N})$ is that the maximum $[\text{La}/\text{Y}]$ value attained with different ^{13}C -efficiencies is reduced to about 0.5. Moreover, with a calibrated extra $X(^{13}\text{C})$ in the tails of the pocket, the maximum $[\text{Pb}/\text{La}]$ is reduced to 1.4 dex. Comparison between theory and observations

Table 1. Envelope abundances of [Y/Fe], [La/Fe], [Pb/Fe] and their ratios, [La/Y] and [Pb/La], for a post-processing model of $M = 2 M_{\odot}$ and $[\text{Fe}/\text{H}] = -2.3$ and various ^{13}C -pocket efficiencies (from $\text{ST} \times 2$ down to $\text{ST}/24$). The first group lists the results obtained with the standard ^{13}C -pocket, while in the second group a further fourth zone with $X(^{13}\text{C}) < X(^{14}\text{N})$ is added.

Cases		$\text{ST} \times 2$	ST	ST/1.5	ST/2	ST/6	ST/12	ST/24
	[Y/Fe]	1.68	1.39	1.33	1.35	1.98	2.35	2.45
	[La/Fe]	2.18	1.88	1.92	2.10	2.85	2.94	2.71
	[Pb/Fe]	4.22	4.12	4.09	4.06	3.82	3.44	2.69
	[La/Y]	0.50	0.49	0.59	0.75	0.87	0.59	0.26
	[Pb/La]	2.04	2.24	2.17	1.96	0.97	0.50	-0.02
	$X(^{13}\text{C})=$	7.2E-2	3.7E-2	2.5E-2	1.9E-2	6.2E-3	3.1E-3	1.6E-3
	$X(^{14}\text{N})=$	2.7E-1	1.4E-1	9.3E-2	7.1E-2	2.3E-2	1.2E-2	5.8E-3
zone 4	[Y/Fe]	1.58	1.75	1.89	2.00	2.40	2.58	2.64
$X(^{13}\text{C}) < X(^{14}\text{N})$	[La/Fe]	2.10	2.25	2.42	2.54	2.92	2.97	2.80
	[Pb/Fe]	4.04	4.02	3.99	3.97	3.76	3.43	2.84
	[La/Y]	0.52	0.50	0.53	0.54	0.52	0.39	0.16
	[Pb/La]	1.94	1.77	1.57	1.43	0.84	0.46	0.04

Table 2. The same as Table 1, but for a case $\text{ST} \times 2$ and an added fourth zone with different $X(^{13}\text{C})$ values, from 0 (standard case) up to 4.3×10^{-3} . $X(^{14}\text{N})$ is assumed to be negligible. In the last column the results obtained by C09 are listed.

zone 4,	standard	I test	II test	III test	IV test	V test	VI test	VII test	C09
$X(^{13}\text{C})$	0.0	2.9E-4	3.5E-4	3.8E-4	4.8E-4	5.8E-4	1.2E-3	4.3E-3	
[Y/Fe]	1.68	2.23	2.21	2.19	2.09	1.97	1.74	1.75	1.12
[La/Fe]	2.18	2.60	2.65	2.75	2.80	2.76	2.48	2.27	1.57
[Pb/Fe]	4.22	4.21	4.23	4.22	4.23	4.24	4.29	4.33	2.88
[La/Y]	0.50	0.37	0.44	0.56	0.71	0.79	0.74	0.52	0.45
[Pb/La]	2.04	1.61	1.58	1.47	1.43	1.48	1.81	2.06	1.30

in CEMP- s stars is then needed in order to constrain the choice of the H profile in the central and outer regions of the ^{13}C -pocket during AGB nucleosynthesis.

Acknowledgements. We are grateful to Roberto Gallino for helpful comments and discussions.

References

- Bisterzo, S., Gallino, R., Straniero, O., Cristallo, S., Käppeler, F. 2010, MNRAS, 404, 1529
- Campbell, S. W., & Lattanzio, J. C. 2008, A&A, 490, 769
- Cristallo, S., Straniero, O., Gallino, R., et al. 2009, ApJ, 696, 797 [C09]
- Denissenkov, P. A., & Tout, C. A. 2003, MNRAS, 340, 722
- Gallino, R., Arlandini, C., Busso, M., et al. 1998, ApJ, 497, 388
- Goriely, S., & Mowlavi, N. 2000, A&A, 362, 599
- Herwig, F., Blöcker, T., Schönberner, D., El Eid, M. 1997, A&A, 324, L81
- Herwig, F., Langer, N., Lugaro, M. 2003, ApJ, 593, 1056
- Karakas, A., & Lattanzio, J. 2003, PASA, 20, 279

- Karakas, A., & Lattanzio, J. 2007, *PASA*, 24, 103
- Iben, I. Jr., & Renzini, A. 1982, *ApJ*, 259, L79
- Langer, N., Heger, A., Wellstein, S., Herwig, F. 1999, *A&A*, 346, L37
- Siess, L., Goriely, S., & Langer, N. 2004, *A&A*, 415, 1089
- Straniero, O., Gallino, R., Busso, M., et al. 1995, *ApJ*, 440, 85
- Straniero, O., Domínguez, I., Cristallo, S., Gallino, R. 2003, *PASA*, 20, 389.
- Straniero, O., Gallino, R., & Cristallo, S. 2006, *Nucl. Phys. A*, 777, 311